Transient natural convection in a square cavity of a fluid with temperature-dependent viscosity

Jae Min Hyun* and Jin Wook Lee
Department of Mechanical Engineering, Korea Advanced Institute of Science and Technology, Chong Ryang, Seoul, Korea

Received March 1987 and accepted for publication July 1987

A study is made of unsteady natural convection in a square cavity of a fluid with a temperature-dependent viscosity. The flow is driven by instantaneously raising the temperature at one vertical wall and lowering the other. The viscosity variation is modeled by an exponential form, $\nu/\nu_0 = \exp(-CT)$. Two boundary conditions at the horizontal walls are used: insulating walls and highly conducting walls. Numerical solutions to the governing time-dependent equations at large reference Rayleigh numbers are acquired. The evolutions of the flow patterns and isotherms are presented under various parameter settings. When the viscosity variations are large, convective activities are facilitated in the region of low viscosity and suppressed in the region of high viscosity. The global impact is to enhance the flow and heat transfer in the cavity. A representative time history of the velocities is shown. A heatup time scale is corroborated. The transient behavior of the Nusselt number at the walls is scrutinized. During the transient phase, the effect of variable viscosity is such that the heat inflow to the cavity exceeds the heat outflow from the cavity. In effect, the cavity acts as a receiver of net heat input during the transient process.

Keywords: transient convection; variable-viscosity fluid; heat transfer node

Introduction

Unsteady natural convection in a cavity has drawn much interest lately. The flow and heat transfer characteristics for large Rayleigh numbers are of interest for a host of thermal engineering applications. One benchmark problem is to determine the flow and temperature fields in a rectangle when the temperature on one vertical wall is lowered and that on the other vertical wall is raised instantaneously. The resulting transient convective motions caused by the differential heating have been studied recently (see, e.g., Patterson and Imberger,[1] Patterson,[2] Kimura and Bejan,[3] Ivey,[4] Hyun[5,6]). The flow is established by the density gradient perpendicular to the direction of gravity. As observed by Ostrach,[7] this type of "heated-by-sidewalls" convective flow occurs frequently in engineering applications as well as in environmental fluid systems. Also, this flow configuration encompasses the fundamental dynamic elements central to a proper understanding of the unsteady convective process.

The majority of the previous work on unsteady internal convection has dealt with the situations in which the thermophysical properties of the fluid have been taken to be constant. It is well known that, in certain fluid systems of practical importance, the variation of viscosity with temperature is substantial, whereas other properties are far less sensitive to the flow conditions (see, e.g, Booker[8]). The effects of strong variations of viscosity on steady-state convection were studied by a few authors. Notably, Booker[8] and Torrance and Turcotte[9] considered steady convection in a horizontal layer heated from below; Yamasaki and Irvine[10] examined steady convection in a vertical tube. These studies have demonstrated that the effects of variable viscosity significantly influence the flow and heat transfer characteristics.

We intend in this paper to investigate the effects of a variable viscosity on unsteady natural convection in a differentially heated rectangle. To isolate the effects of a temperature-dependent viscosity, we adopt a square cavity. We seek numerical solutions to the governing Navier-Stokes equation. The variability of viscosity is modeled by a simple, yet widely exploited, formulae.[9] The comprehensive transient data of the flow and temperature fields is monitored for two cases of the thermal boundary condition at the horizontal walls: insulated walls and when the wall temperature varies linearly between the two vertical walls.

We illuminate the details of the flow and thermal structures inside the cavity as the reference Rayleigh number and the temperature dependency of viscosity are varied. The effects of the reference Prandtl number and of the cavity aspect ratio will be treated in a subsequent paper.

The key results are the time-dependent stream patterns and isotherms. The thermal stratification in the interior core will show different character as the horizontal wall boundary conditions are altered. The overall impact of a strongly variable viscosity on the global convective motions is scrutinized. Of particular interest are the transient variations of the Nusselt numbers on the boundary walls. With variable viscosity, the influence of convection is larger in the regions of low viscosity. The corresponding resulting variations in the heat transfer characteristics near the walls point to a possibility that, during the transient phase, there can be a net heat input to the cavity. The behavior of the mean Nusselt numbers on the walls is examined for various values of the external parameters.

* To whom correspondence should be addressed.

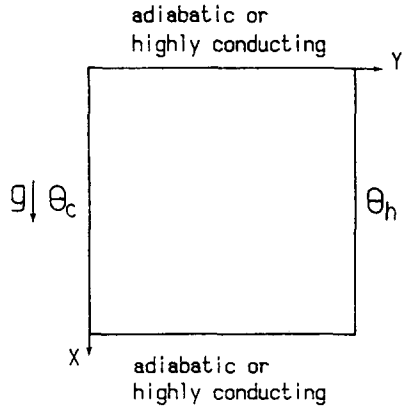

Figure 1 Flow configuration and coordinate system

Formulation

The flow configuration of interest is shown in Figure 1. A square cavity is filled with an incompressible, Boussinesq-type, viscous fluid. Cartesian coordinates (x, y) are used, and the corresponding velocity components are denoted by (u, v). Initially, the fluid is motionless and at a uniform temperature θ_0. At the initial moment $t=0$, the temperature on the left vertical sidewall is lowered to θ_c, and that in the right vertical sidewall is raised to θ_h. These sidewall temperatures are maintained thereafter. For simplicity, we consider the case $\theta_0=(\theta_c+\theta_h)/2$. Two kinds of thermal boundary conditions for the horizontal walls are specified: an insulated condition, and a linearly varying temperature condition $\theta=\theta_c+(\theta_h-\theta_c)y/d$.

The governing equations, written in vorticity (ζ) stream function (ψ) formulation are, in a properly nondimensionalized form (see e.g., Yamasaki and Irvine[10]),

$$\frac{\partial U}{\partial X}+\frac{\partial V}{\partial Y}=0 \tag{1}$$

$$\frac{\partial T}{\partial t}+U\frac{\partial T}{\partial X}+V\frac{\partial T}{\partial Y}=\frac{1}{\mathrm{Pr}_0}\left(\frac{\partial^2 T}{\partial X^2}+\frac{\partial^2 T}{\partial Y^2}\right) \tag{2}$$

$$\frac{\partial \zeta}{\partial t}+U\frac{\partial \zeta}{\partial X}+V\frac{\partial \zeta}{\partial Y}=\mathrm{Gr}_0\frac{\partial T}{\partial Y}+\nabla^2(\pi\zeta)+2\left[\frac{\partial^2\pi}{\partial X^2}\frac{\partial U}{\partial Y}-\frac{\partial^2\pi}{\partial Y^2}\frac{\partial V}{\partial X}+\frac{\partial^2\pi}{\partial X\partial Y}\left(\frac{\partial V}{\partial Y}-\frac{\partial U}{\partial X}\right)\right] \tag{3}$$

$$\nabla^2\psi=-\zeta \tag{4}$$

$$U=\frac{\partial\psi}{\partial Y},\qquad V=-\frac{\partial\psi}{\partial X} \tag{5}$$

where the nondimensional quantities are defined as follows:

$$X=\frac{x}{d},\quad Y=\frac{y}{d},\quad U=\frac{u}{\nu_0/d},\quad V=\frac{v}{\nu_0/d}$$

$$T=\frac{\theta-\theta_0}{\theta_h-\theta_c},\quad \mathrm{Pr}_0=\frac{\nu_0}{\kappa},\quad \mathrm{Gr}_0=\frac{g\beta\Delta\theta d^3}{\nu_0^2} \tag{6}$$

$$\pi=\frac{\nu}{\nu_0},\quad t=\frac{t^*}{d^2/\nu_0}$$

In the above, the relevant fluid properties are kinematic viscosity ν, thermal diffusivity κ, and coefficient of volumetric expansion β. The kinematic viscosity at the initial uniform temperature is denoted by ν_0. The important reference nondimensional parameters are the Prandtl number Pr_0, the Grashof number Gr_0, and the Rayleigh number $\mathrm{Ra}_0=\mathrm{Gr}_0\,\mathrm{Pr}_0$. Note that dissipation has been neglected in the energy equation.

The variability of viscosity is denoted by π, which is the viscosity ratio referred to the reference value ν_0. We adopt a simple exponential form proposed by Torrance and Turcotte:[9]

$$\pi=\exp(-CT) \tag{7}$$

Obviously, $C=0$ corresponds to the constant-viscosity case. This exponential model for the viscosity-temperature relation describes the available experimental data reasonably well (Booker,[8] Yamasaki and Irvine[10]). References 8–10 choose a form similar to that given by Equation 7.

In accordance with the problem statement, the initial conditions are

$$U=V=T=0 \tag{8}$$

The appropriate boundary conditions are

$$U=V=0 \quad \text{on all solid boundaries}$$

$$T=-0.5 \quad \text{on } Y=0,\qquad T=0.5 \quad \text{on } Y=1$$

$$\frac{\partial T}{\partial X}=0 \quad \text{on } X=0,1 \quad \text{(adiabatic horizontal walls)}$$

$$T=Y-0.5 \quad \text{on } X=0,1 \quad \text{(conducting horizontal walls)} \tag{9}$$

Our task is to solve the system of coupled differential equations (1)–(9). We obtained the numerical solutions to these equations by using the finite difference numerical methods originally

Notation

C	Viscosity variation parameter
C_p	Specific heat
d	Width of cavity
Gr_0	Reference Grashof number, $g\beta\Delta\theta d^3/\nu_0^2$
k	Thermal conductivity
NU	Average Nusselt number at boundary wall
Pr	Reference Prandtl number, ν_0/κ
Q	Heat flow at boundary wall
Ra_0	Reference Rayleigh number, $g\beta\Delta\theta d^3/\kappa\nu_0$
t, t^*	Nondimensional, dimensional time
T	Nondimensional temperature
u, v	Velocity components
U, V	Nondimensional velocity components
x, y	Coordinates
X, Y	Nondimensional coordinates

Greek symbols

β	Coefficient of volumetric expansion
ζ	Nondimensional vorticity
θ	Dimensional temperature
κ	Thermal diffusivity, $k/\rho C_p$
ν_0	Reference kinematic viscosity
ν	Local kinematic viscosity
π	Normalized kinematic viscosity, ν/ν_0
ρ	Density
ψ	Nondimensional stream function

Subscripts

0	Reference value
c	Cold wall
h	Hot wall
t	Top wall
b	Bottom wall

developed by Wilkes and Churchill.[11] We integrated the equations at discrete time steps by the alternating direction implicit numerical procedures. For full details of numerical techniques, see Ref. 11. The mesh points used were typically 21×21 to 26×26. We performed sensitivity tests to the grid size for several sample runs by repeating the calculations on finer grids. The results were found to be in satisfactory agreement with each other, providing credence to the mesh size that we had selected. As stated earlier, we confined our attention to the effects of variable viscosity. The cavity aspect ratio was fixed at unity, and the reference Prandtl number Pr_0 was set at 7.0. Numerical computations were executed by using several values of C in Equation 7 over a range of the reference Rayleigh number Ra_0.

Results and discussion

At first we shall be concerned with the results obtained by using the adiabatic horizontal wall conditions. Figures 2 and 3 illustrate the transient evolution of flow and temperature fields for a constant-viscosity fluid ($C=0$) at two values of Ra_0. These plots will serve as standards to assess the effects of a variable viscosity. Also, the results in Figures 2 and 3 are checked against the results of others who used different numerical techniques. This will verify the accuracy and reliability of the present numerical model.

Figure 2, at a lower value of Ra_0, demonstrates that, immediately after the impulsive start, two secondary rolls appear inside the primary circulation. At small times, the convective motions have not fully developed. Therefore, in thin boundary layers on the vertical walls, the isotherms are crowded

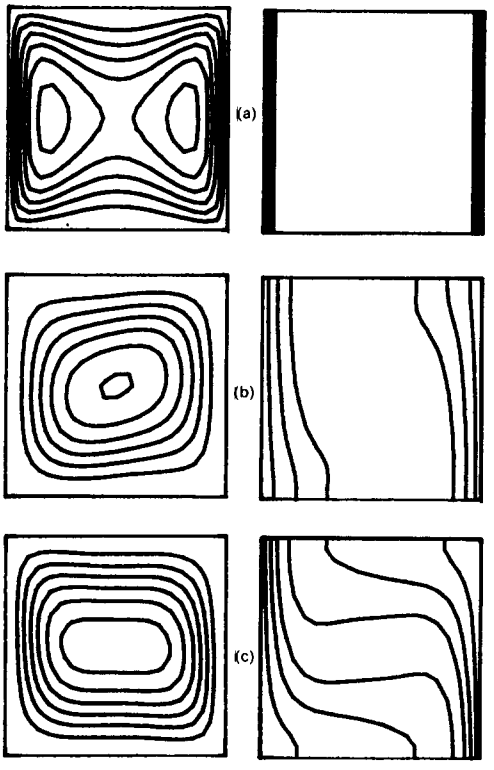

Figure 2 Plots of stream function (left column) and isotherms (right column) in the cavity. $Ra_0=3.5\times10^4$, $C=0$. Adiabatic horizontal walls. Times are (a) $t=0.003$, (b) $t=0.07$, (c) $t=1.5$. Values for ψ in the figures are (a) $\psi_{max}=0.105$, contour increment $\Delta\psi=0.0175$; (b) $\psi_{max}=1.8$, $\Delta\psi=0.3$; (c) $\psi_{max}=1.05$, $\Delta\psi=0.175$. Isotherms are, from left to right, -0.4, -0.25, -0.1, 0.1, 0.25, 0.4

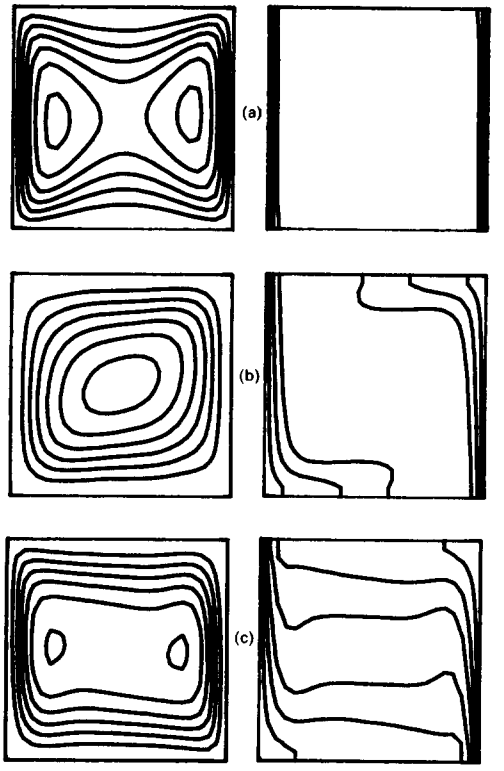

Figure 3 Plots of stream function (left column) and isotherms (right column) in the cavity. $Ra_0=3.5\times10^5$, $C=0$. Adiabatic horizontal walls. Times are (a) $t=0.003$, (b) $t=0.04$, (c) $t=1.5$. Values for ψ in the figures are (a) $\psi_{max}=0.9$, contour increment $\Delta\psi=0.15$; (b) $\psi_{max}=6.0$, $\Delta\psi=1.0$; (c) $\psi_{max}=2.1$, $\Delta\psi=0.35$. Isotherms are, from left to right, -0.4, -0.25, -0.1, 0.1, 0.25, 0.4

and approximately parallel to the vertical walls; this is indicative of the dominance of conduction. The bulk of the fluid is still at the initial temperature $T=0$ (see Figure 2(a)).

The flows subsequently grow in magnitude to their peak values, suggesting that the fluid is accelerating. At intermediate times, the two rolls merge into a single circulatory pattern. Owing to the intensified convective motions, the temperature field in the interior begins to be stratified in the vertical direction (see Figure 2(b)). After reaching the peak values, the fluid decelerates slightly and approaches the steady state.

At large times, the flow tends slowly to the established final state; the convective circulatory pattern fills in much of the cavity. In the inviscid interior core, the predominant vertical stratification is discernible. The plots shown in Figure 2(c) can be taken to depict the steady state. Here, for computational purposes, the steady state will be defined as the state when the flow variables vary less than a prescribed amount over a physically meaningful time interval. For flows of large Rayleigh numbers, one significant time scale is the heatup time scale $\tau \sim Ra^{-1/4}$ (Patterson and Imberger,[1] Hyun[5,6]). Therefore, we regard the steady state to have been achieved if the temporal variations of the flow variables are less than 0.1% over a time interval of $0.1Ra_0^{-1/4}$. Additional discussion on the approach to the steady state will be given in connection with the behavior of the mean Nusselt numbers on the two vertical sidewalls.

Figure 3 displays the results at higher Ra_0. The overall patterns of transient evolution are qualitatively similar to those shown in Figure 2. One notable difference is seen in the flow structure at large times. In Figure 3(c), the secondary rolls reappear, in contrast to the flow pattern shown in Figure 2(c). These features were also observed in previous studies (Elder[12]).

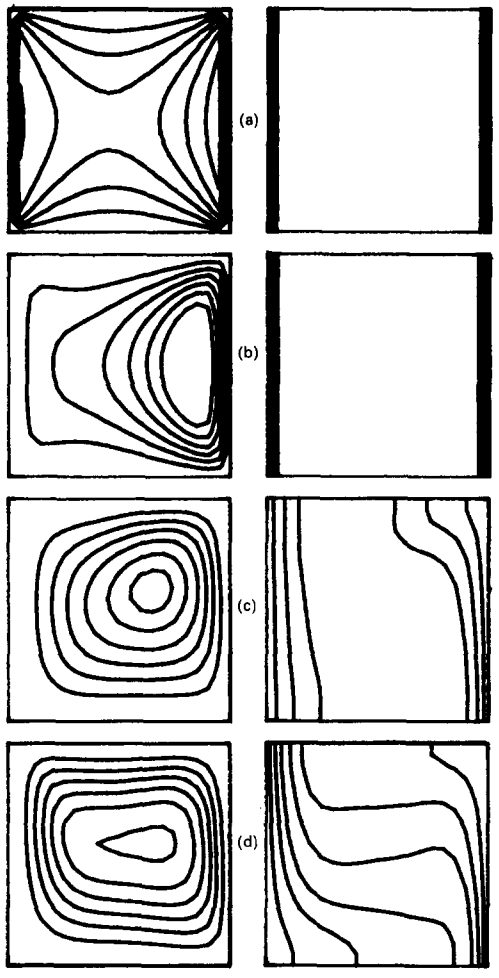

Figure 4 Plots of stream function (left column) and isotherms (right column) in the cavity. $Ra_0=3.5\times10^4$, $C=3$. Adiabatic horizontal walls. Times are (a) $t=0.00004$, (b) $t=0.003$, (c) $t=0.07$, (d) $t=1.5$. Values for ψ in the figures are (a) $\psi_{max}=0.006$, contour increment $\Delta\psi=0.001$; (b) $\psi_{max}=0.18$, $\Delta\psi=0.03$; (c) 0.35, 0.7, 1.05, 1.4, 1.75, 2.0; (d) $\psi_{max}=1.2$, $\Delta\psi=0.2$. Isotherms are, from left to right, -0.4, -0.25, -0.1, 0.1, 0.25, 0.4

It is presumed that, at lower Ra_0, the relative importance of viscous diffusion outweighs the effect of the negative $\partial T/\partial Y$ near the center of the cavity; therefore, the development of the secondary rolls is retarded by the diffusive effects. The qualitative features shown in Figures 2 and 3 exemplify the unsteady convective process of a constant viscosity fluid at large Rayleigh numbers; these have been well documented (see, e.g., Wilkes and Churchill,[11] Küblbeck *et al.*[13]).

We now examine the explicit effect of a temperature-dependent viscosity. With the assumed form of Equation 7, numerical solutions were generated using $C=1,3,7$ at two values of Ra_0.The viscosity is a maximum at the cold vertical wall and a minimum at the hot vertical wall.

The results of the computations for a strongly variable viscosity ($C=3$) are shown in Figures 4 and 5. Comparisons of the circulation patterns and isotherms for $C=0$ and those described in Figures 4 and 5 reveal considerable changes. When $C\neq0$, near the hot wall, viscosity is lowered and the flow intensifies; near the cold wall, viscosity increases and the flow is suppressed. However, the former outweighs the latter, and the global impact is to enhance the overall convective activities in the cavity. Clearly, the flow is concentrated in the region of low viscosity. At a lower value of Ra_0, the location of ψ_{max} moves toward the region of lowest viscosity. Near the upper right corner of the cavity, the temperature is highest owing to the rising fluid in the boundary layer on the hot vertical wall; this is the region of lowest viscosity. The isotherms near the cold wall in Figures 4(c) and 5(c) tend to be more nearly parallel than those near the hot wall. This reflects the fact that conduction has appreciable influence in the region of high viscosity. The general characteristics described above are representative of all the results obtained by using other nonzero values of C, and these results are not reproduced here.

At a large value of Ra_0 (see Figure 5), as for a constant-viscosity fluid (see Figure 3), the secondary rolls merge at small times and reappear at large times. A perusal of the entire set of the results indicates that as C increases, the merging of the secondary rolls takes place earlier, and the re-formation of the secondary rolls is delayed to a still later time.

As Ra_0 increases, the thickness of the boundary layers near the vertical walls decreases. Large positive values of $\partial T/\partial Y$ are seen near the upper region of the cold wall and the lower region of the hot wall. The convective motions are vigorous in these regions. As C increases, the magnitude of vorticity near the hot wall exceeds that near the cold wall. A larger secondary roll is apparent near the hot wall (see Figure 5(d)).

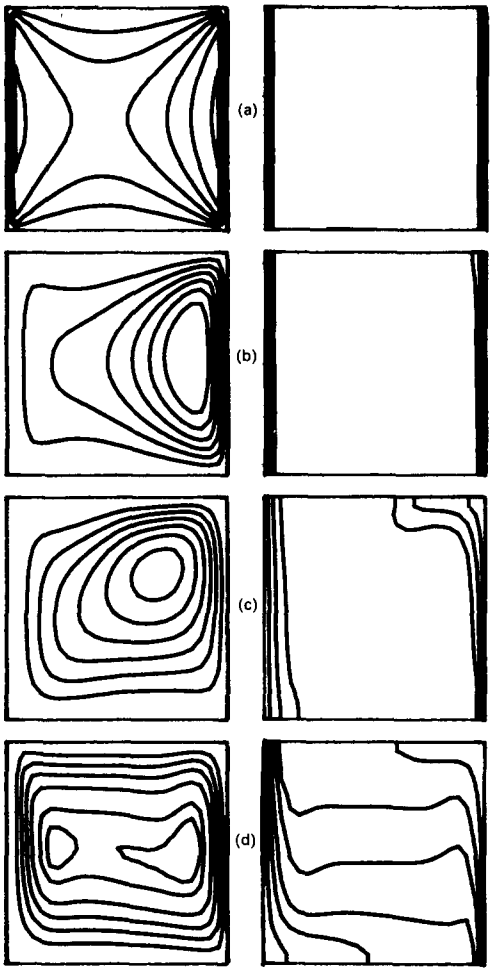

Figure 5 Plots of stream function (left column) and isotherms (right column) in the cavity. $Ra_0=3.5\times10^5$, $C=3$. Adiabatic horizontal walls. Times are (a) $t=0.00004$, (b) $t=0.003$, (c) $t=0.02$, (d) $t=1.5$. Values for ψ in the figures are (a) $\psi_{max}=0.051$, contour increment $\Delta\psi=0.0085$; (b) $\psi_{max}=1.5$, $\Delta\psi=0.25$; (c) $\psi_{max}=6.0$, $\Delta\psi=1.0$; (d) 0.4, 0.8, 1.2, 1.6, 2.0, 2.15. Isotherms are, from left to right, -0.4, -0.25, -0.1, 0.1, 0.25, 0.4

Table 1 Maximum values of the stream function ψ_{max}. Adiabatic horizontal wall conditions

		$t=0.07$	Steady state
$Ra_0=3.5\times10^4$	$C=0$	1.832	1.155
	1	1.885	1.165
	3	2.112	1.240
	7	2.621	1.549
$Ra_0=3.5\times10^5$	0	3.864	2.135
	1	4.039	2.156
	3	4.256	2.256
	7	4.677	2.710

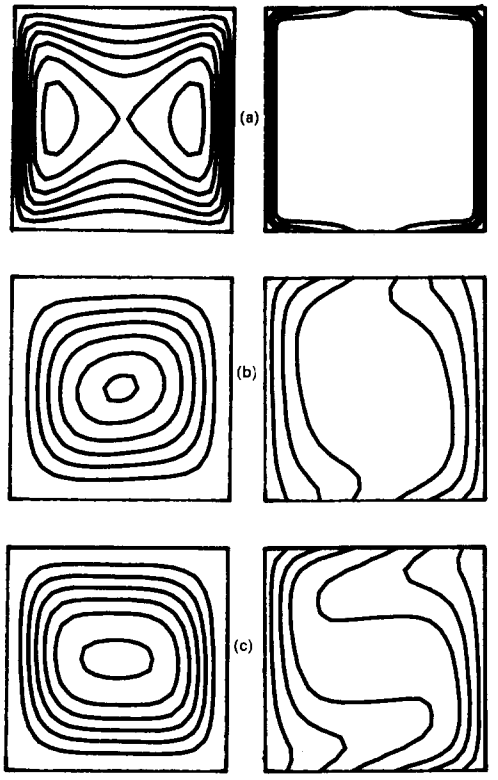

Figure 6 Plots of stream function (left column) and isotherms (right column) in the cavity. $Ra_0=3.5\times10^4$, $C=0$. Conducting horizontal walls. Times are (a) $t=0.003$, (b) $t=0.07$, (c) $t=1.5$. Values for ψ in the figures are (a) $\psi_{max}=0.105$, contour increment $\Delta\psi=0.0175$; (b) 0.35, 0.7, 1.05, 1.4, 1.75, 2.0; (c) 0.25, 0.5, 0.75, 1.0, 1.25, 1.55. Isotherms are, from left to right, -0.4, -0.25, -0.1, 0.1, 0.25, 0.4

In summary, a systematic inspection of the results points to the following important observations. In a variable-viscosity fluid, the convective motions inside the cavity are more vigorous than for a constant-viscosity fluid. The flow enhancement due to the decrease of viscosity near the hot wall surpasses the flow suppression due to the increase of viscosity near the cold wall. This effect is better manifested by comparing ψ_{max}, which is listed in Table 1.

We next turn to the cases when the horizontal walls are highly conducting; the temperatures on the horizontal walls are linearly varying between the two vertical isothermal walls. As pointed out by Briggs and Jones,[14] this conducting-wall boundary condition has received less attention in the literature, although the problem is inherently of much relevance to technological applications.

Figures 6 and 7 illustrate the plots of stream functions and isotherms for a constant-viscosity fluid. Comparing these results with those for the case of insulated walls, we see that differences are more apparent in the thermal structures than in the flow patterns. At small times, conduction layers are formed on the horizontal walls as well as on the vertical walls (see Figures 6(a) and 7(a)). The flow intensifies to its peak magnitude at intermediate times. The flow decreases in magnitude slightly afterward, and it tends smoothly to the steady state. The heat transfer between the fluid and the horizontal walls augments the overall convective activities. In the steady state, the interior core, in which a predominant vertical stratification exists, occupies a smaller portion of the cavity than for the case of insulating walls. Considerable portions of the cavity near the horizontal walls are characterized by an appreciable horizontal stratification, owing to the imposed horizontal wall boundary conditions (see Figures 6(c) and 7(c)).

Figures 8 and 9 depict the stream patterns and isotherms for a strongly variable viscosity fluid. The concentration of flow in the regions of low viscosity is discernible. At large times, the isotherms in the regions close to the solid boundaries point to the existence of patches of gravitationally unstable configuration; (i.e., a cold fluid overlies hot fluid (see Figure 9(d)).

Since the viscosity varies by substantial margins in the cavity, Ra_0 based on ν_0, may not fully characterize the localized phenomena. Especially in the upper region near the hot wall, viscosity is the lowest; therefore, the effective Rayleigh number is very large. Accordingly, the local behavior in that region may be characteristic of the convection at a Rayleigh number higher than Ra_0.

In summary, the highly conducting horizontal walls facilitate the global convective activities in the cavity. A comparison of

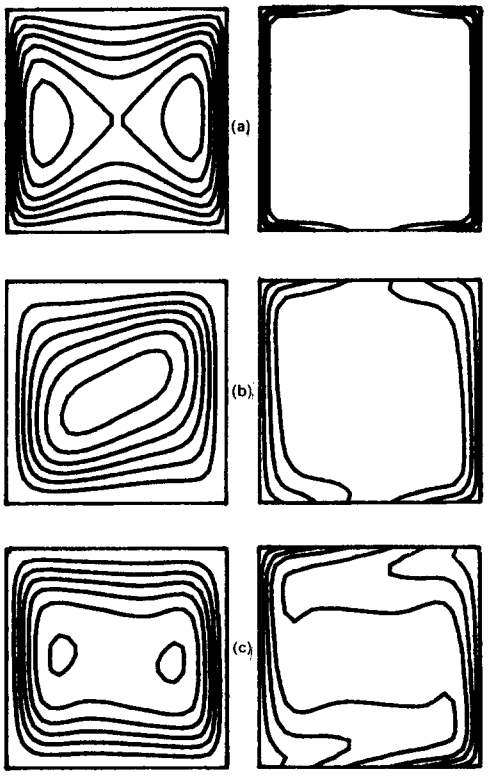

Figure 7 Plots of stream function (left column) and isotherms (right column) in the cavity. $Ra_0=3.5\times10^5$, $C=0$. Conducting horizontal walls. Times are (a) $t=0.003$, (b) $t=0.02$, (c) $t=1.5$. Values for ψ in the figures are (a) $\psi_{max}=0.9$, contour increment $\Delta\psi=0.15$; (b) $\psi_{max}=4.8$, $\Delta\psi=0.8$; (c) $\psi_{max}=3.0$, $\Delta\psi=0.5$. Isotherms are, from left to right, -0.4, -0.25, -0.1, 0.1, 0.25, 0.4

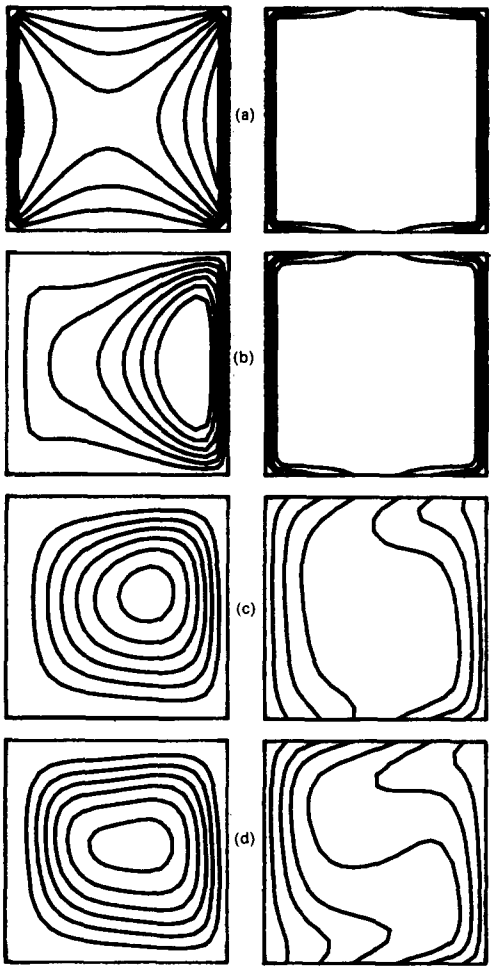

Figure 8 Plots of stream function (left column) and isotherms (right column) in the cavity. $Ra_0=3.5\times10^4$, $C=3$. Conducting horizontal walls. Times are (a) $t=0.00004$, (b) $t=0.003$, (c) $t=0.07$, (d) $t=1.5$. Values for ψ in the figures are (a) $\psi_{max}=0.006$, contour increment $\Delta\psi=0.001$; (b) $\psi_{max}=0.18$, $\Delta\psi=0.03$; (c) $\psi_{max}=2.1$, $\Delta\psi=0.35$; (d) 0.27, 0.54, 0.81, 1.08, 1.35, 1.6. Isotherms are, from left to right, -0.4, -0.25, -0.1, 0.1, 0.25, 0.4

the values of ψ_{max} for the insulating walls (Table 1) and for the conducting walls (Table 2) clearly bears this out.

Figure 10 demonstrates a typical time history of the velocity components. As stated earlier, the fluid accelerates from the initial motionless state to the peak value; afterward, the fluid decelerates slightly and proceeds smoothly to its steady-state limit. The time span over which the fluid motion, starting from zero, tends to the steady state (i.e., for example, the velocity reaches within 10% of the steady-state value) is significant in the transient adjustment process. This will be a measure of the time over which the convective motions have been substantially adjusted. Patterson and Imberger[1] and Hyun[5,6] showed that this heatup time was scaled with $O(Ra^{-1/4})$. The exemplary time-history plots in Figure 10 are consistent with this scaling.

The variations of the mean heat transfer coefficient NU at the cavity walls are depicted in Figures 11 and 12. Here, the Nusselt number NU is computed as

$$NU=\int_0^1\left(\frac{\partial T}{\partial Y}\right)_{T=0,1}dX$$

for the vertical walls, and

$$NU=\int_0^1\left(\frac{\partial T}{\partial X}\right)_{X=0,1}dY$$

for the horizontal walls in the case of conducting walls.

Figure 11 presents the results for the case of insulated horizontal walls. For a flow with constant viscosity (see Figure 11(a)), the influence of convection becomes effective only at some small time after the impulsive start. As expounded by Wilkes and Churchill,[11] this is due to the lapse of time occurring while the fluid travels through the cavity between the two vertical walls. It is important to recognize that for a constant-viscosity fluid, the Nusselt numbers at the two vertical walls are identical at all times; no heat is accumulated in the cavity during the entire process. This is anticipated, since no energy dissipation or production has been included in the formulation. As is clear in Figure 11(f), the steady-state isotherm for $T=0$ for $C=0$ divides the cavity evenly; $T>0$ in the upper right region and $T<0$ in the lower left region. These salient features for a constant-viscosity fluid were captured previously.[11]

The Nusselt numbers at the vertical walls are profoundly affected by the effect of variable viscosity. As C increases, NU at the hot wall is significantly larger than NU at the cold wall during the transient phase. Near the hot wall, viscosity is

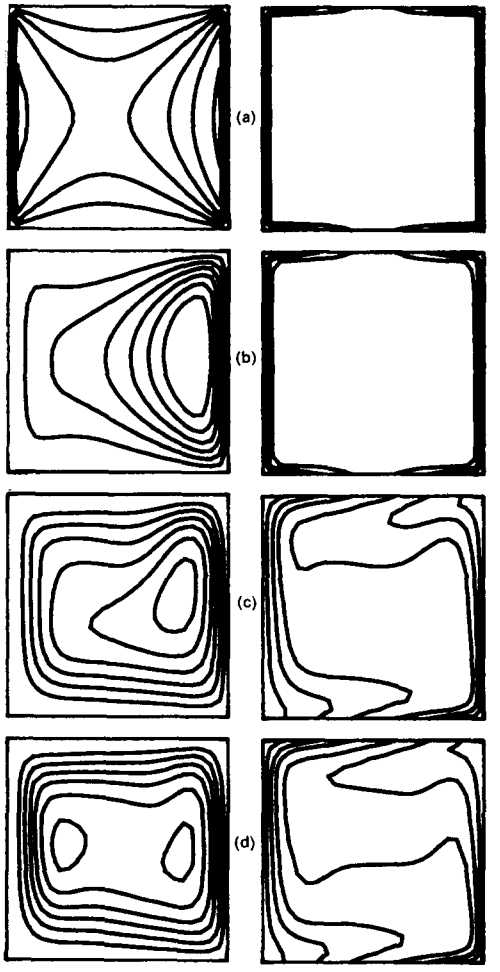

Figure 9 Plots of stream function (left column) and isotherms (right column) in the cavity. $Ra_0=3.5\times10^5$, $C=3$. Conducting horizontal walls. Times are (a) $t=0.00004$, (b) $t=0.003$, (c) $t=0.07$, (d) $t=1.5$. Values for ψ in the figures are (a) $\psi_{max}=0.051$, contour increment $\Delta\psi=0.0085$; (b) $\psi_{max}=1.5$, $\Delta\psi=0.25$; (c) $\psi_{max}=4.2$, $\Delta\psi=0.7$; (d) 0.56, 1.12, 1.68, 2.24, 2.7, 3.1. Isotherms are, from left to right, -0.4, -0.25, -0.1, 0.1, 0.25, 0.4

reduced substantially; convection sets in earlier, and the dominance of convection prevails in a larger region than for $C=0$. Near the cold wall, the opposite effects take hold. However, the former outweighs the latter. In effect, the cavity can be regarded as a receiver of a net heat input during the transient phase. This net heat added to the cavity during the transient phase has enabled the steady state to sustain the thermal structure shown in Figure 11(f). Only at the steady state the flow becomes settled, and the Nusselt numbers at the two vertical walls are equalized. In the steady state, the upper right region ($T>0$) is larger than the lower left region ($T<0$). In essence, the global heat content in the cavity at the steady state is larger than that of the initial state.

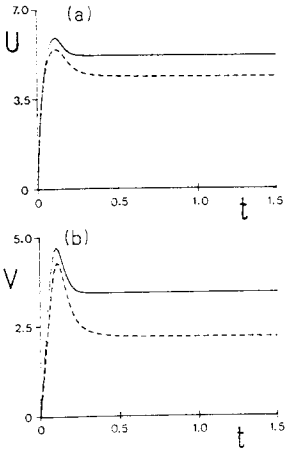

Figure 10 Representative time history of the velocities for $Ra_0=3.5\times10^4$, $C=0$. (a) Vertical velocity at $X=0.5$, $Y=0.95$; (b) horizontal velocity at $X=0.95$, $Y=0.5$; – – – –: adiabatic horizontal walls; ——: conducting horizontal walls

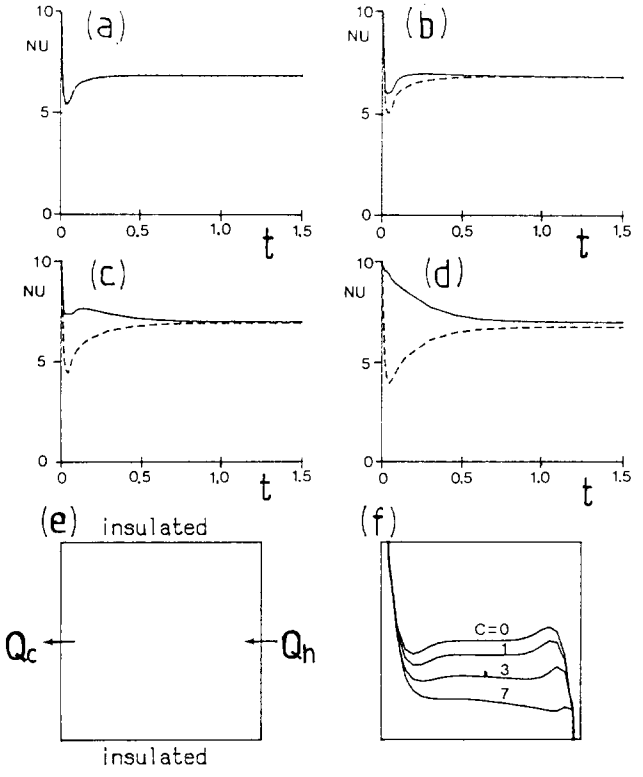

Figure 11 Variation of the mean Nusselt numbers. (a) $C=0$; (b) $C=1$; (c) $C=3$; (d) $C=7$; (e) heat transfer along the walls; (f) the locations of the isotherm for $T=0$ at $t=1.5$. $Ra_0=3.5\times10^5$. Adiabatic horizontal walls; – – – –: at cold wall; ——: at hot wall

Table 2 Maximum values of the stream function ψ_{max}. Conducting horizontal wall conditions

		$t=0.07$	Steady state
$Ra_0=3.5\times10^4$	$C=0$	2.043	1.617
	1	2.090	1.634
	3	2.294	1.710
	7	2.708	2.168
$Ra_0=3.5\times10^5$	0	4.006	3.069
	1	4.202	3.088
	3	4.568	3.189
	7	5.317	3.918

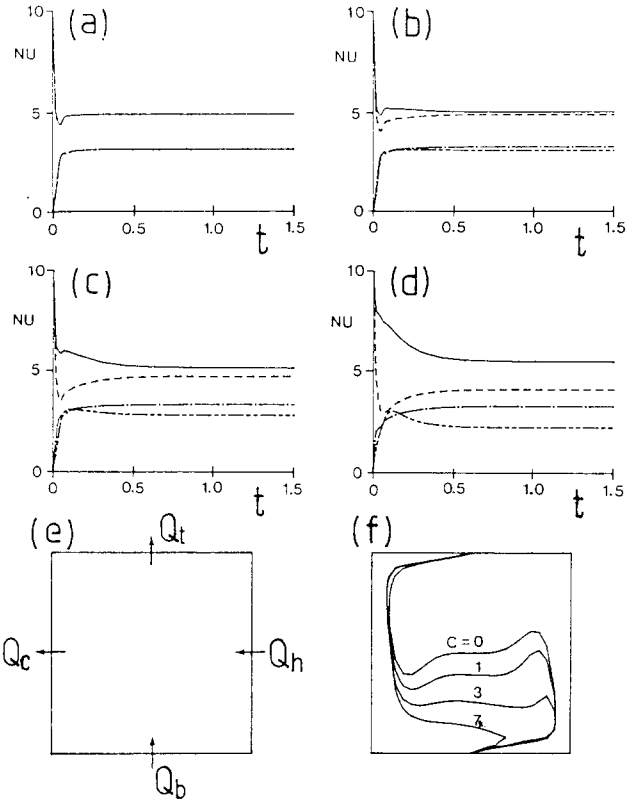

Figure 12 Variation of the mean Nusselt numbers. (a) $C=0$; (b) $C=1$; (c) $C=3$; (d) $C=7$; (e) heat transfer along the walls; (f) the locations of the isotherm for $T=0$ at $t=1.5$. $Ra_0=3.5\times10^5$. Conducting horizontal walls; – – – –: at cold wall; ——: at hot wall; —·—·—: at top wall; —··—··—: at bottom wall

Figure 12 is for the case of conducting horizontal walls. The fluid exchanges heat along the four boundaries of the cavity, as shown in Figure 12(e). For a constant-viscosity fluid, $Q_h=Q_c$ and $Q_b=Q_t$ at all times; there is no net heat addition to the cavity. The transient behavior is qualitatively similar to that in Figure 11(a).

The effect of variable viscosity affects measurably the Nusselt numbers at the four boundary walls. As C increases, convective activities are intensified in the region of low viscosity and suppressed in the region of high viscosity. During the transient phase, the heat inflow to the cavity, Q_h+Q_b, is larger than the heat outflow from the cavity, Q_c+Q_t, as shown in Figures 12(b), (c), (d). At the steady state, $Q_h+Q_b=Q_c+Q_t$, implying that no net heat is being added to the cavity. Therefore, during the transient phase, there is a net heat input to the cavity.

Accordingly, the heat content in the entire cavity at the steady state is larger than that of the initial state. As seen in Figure 12(f), in the steady state the right region of the cavity where $T>0$ is larger than the left region where $T<0$.

Conclusion

Numerical solutions have been obtained to delineate the effect of variable viscosity on the unsteady process in a square cavity heated differentially at the vertical walls.

With a variable-viscosity fluid, the convective activities are facilitated near the hot wall and suppressed near the cold wall. However, the overall impact is to enhance the flow and heat transfer in the cavity. This effect is more pronounced for conducting horizontal walls.

The flow is substantially adjusted to its steady state features within a heatup time scale $O(\mathrm{Ra}^{-1/4})$. For a constant-viscosity fluid, the Nusselt numbers at the boundary walls are identical at all times. For a variable-viscosity fluid, however, convection is more vigorous near the hot wall. During the transient phase, for insulating horizontal walls, the heat inflow to the cavity at the hot vertical wall exceeds the heat outflow at the cold vertical wall. Therefore, the cavity acts as a receiver of net heat input in a variable-viscosity fluid. For conducting horizontal walls, during the transient phase, the heat inflow through the hot vertical wall and the bottom wall is larger than the heat outflow through the cold vertical wall and the top wall.

Acknowledgments

This work was supported in part by a grant (H03830) from the Korea Science and Engineering Foundation.

References

1 Patterson, J. and Imberger, J. Unsteady natural convection in a rectangular cavity. *J. Fluid Mech.*, 1980, **100**(1), 65–86

2 Patterson, J. On the existence of an oscillatory approach to steady natural convection in cavities. *Trans. Am. Soc. Mech. Engrs. Ser. C, J. Heat Transfer*, 1984, **106**, 104–108

3 Kimura, S. and Bejan, A. The boundary layer natural convection regime in a rectangular cavity with uniform heat flux from the side. *Trans. Am. Soc. Mech. Engrs. Ser. C, J. Heat Transfer*, 1984, **106**, 98–103

4 Ivey, G. N. Experiments on transient natural convection in a cavity. *J. Fluid Mech.*, 1976, **144**, 389–401

5 Hyun, J. M. Transient buoyant convection of a contained fluid driven by the changes in the boundary temperatures. *Trans. Am. Soc. Mech. Engrs. Ser. B, J. Appl. Mech.*, 1985, **52**, 193–198

6 Hyun, J. M. Transient process of thermally stratifying an initially homogeneous fluid in an enclosure. *Int. J. Heat Mass Transfer*, 1984, **27**(10), 1936–1938

7 Ostrach, S. Natural convection heat transfer in cavities and cells. Proc. 7th Int. Heat Transfer Conf., Munich, Vol. 1, pp. 365–379, Hemisphere, Washington, D.C., 1982

8 Booker, J. R. Thermal convection with strongly temperature dependent viscosity. *J. Fluid Mech.*, 1976, **76**(4), 741–754

9 Torrance, K. E. and Turcotte, D. L. Thermal convection with large viscosity variations. *J. Fluid Mech.*, 1971, **47**(1), 113–125

10 Yamasaki, T. and Irvine, T. F. Laminar free convection in a vertical tube with temperature-dependent viscosity. *Int. J. Heat Mass Transfer*, 1984, **27**(9), 1613–1621

11 Wilkes, J. O. and Churchill, S. W. The finite-difference computation of natural convection in a rectangular enclosure. *AIChE J.*, 1966, **12**, 161–166

12 Elder, J. W. Laminar free convection in a vertical slot. *J. Fluid Mech.*, 1965, **23**(1), 78–98

13 Küblbeck, K., Merker, G. P., and Straub, J. Advanced numerical computation of two-dimensional time-dependent free convection in cavities. *Int. J. Heat Mass Transfer*, 1980, **23**, 203–217

14 Briggs, D. G. and Jones, D. N. Two dimensional periodic natural convection in a rectangular enclosure of aspect ratio one. *Trans. Am. Soc. Mech. Engrs. Ser. C, J. Heat Transfer*, 1985, **107**, 850–854